**Atmospheric
Chemistry
and Physics
Discussions**

Size-segregated aerosol mass closure and chemical composition in Monte Cimone (I) during MINATROC

J.-P. Putaud[1], R. Van Dingenen[1], A. Dell'Acqua[1], F. Raes[1], E. Matta[2], S. Decesari[2], M. C. Facchini[2], and S. Fuzzi[2]

[1]European Commission, Joint Research Centre, Institute for Environment and Sustainability, Ispra (Va), Italy
[2]Consiglio Nazionale delle Ricerche, Istituto delle Scienze dell'Atmosfera e del Clima, Bologna, Italy

Correspondence to: J.-P. Putaud (jean.putaud@jrc.it)

Title Page

Abstract   Introduction

Conclusions   References

Tables   Figures

◄◄   ►►

◄   ►

Back   Close

Full Screen / Esc

Print Version

Interactive Discussion

© EGU 2003

Size-segregated aerosol mass closure and chemical composition

J.-P. Putaud et al.

Abstract

Physical and chemical characterizations of the atmospheric aerosol was carried out at Mt. Cimone (Italy) during the 4 June–4 July 2000 period. Particle size distributions in the size range 6 nm-10 μm were measured with a differential mobility analyzer (DMA) and a optical particle counter (OPC). Size-segregated aerosol was sampled using a 6-stage low pressure impactor. Aerosol samples were submitted to gravimetric and chemical analyses. Ionic, carbonaceous and refractory components of the aerosol were quantified. We compared the sub- and super-μm aerosol mass concentrations determined by gravimetric measurements (m_{GM}), chemical analyses (m$_{CA}$), and by converting particle size distribution to aerosol mass concentrations (m_{SD}). Mean random uncertainties associated with the determination of m_{GM}, m$_{CA}$, and m_{SD} were assessed. The three estimates of the sub-μm aerosol mass concentration agreed, which shows that within experimental uncertainty, the sub-μm aerosol was composed of the quantified components. The three estimates of the super-μm aerosol mass concentration did not agree, which indicates that random uncertainties and/or possible systematic errors in aerosol sampling, sizing or analyses were not adequately accounted for. Aerosol chemical composition in air masses from different origins showed differences, which were significant in regard to experimental uncertainties. During the Saharan dust advection period, coarse dust and fine anthropogenic particles were externally mixed. No anthropogenic sulfate could be found in the super-μm dust particles. In contrast, nitrate was shifted towards the aerosol super-μm fraction in presence of desert dust.

1. Introduction

Due to the short atmospheric lifetime and complex chemical composition of atmospheric aerosols, their global distribution shows large regional differences and their radiative properties are poorly known. As a consequence, the radiative forcing by aerosols is the most uncertain, the most heterogeneous, and susceptible to the fastest

changes (IPCC, 2001). Very little is still known about the aerosol forcing related to the effect of particles on the size and number of cloud droplets. Not even best estimates of the current forcing by mineral dust can be given (IPCC, 2001). The parameters controlling the aerosol direct and indirect radiative forcing can be calculated from the aerosol
5 composition as a function of the particle size. Ideally, single particle size, composition, (and shape) should be determined. Recently developed instruments based on aerodynamic sizing and time of flight mass spectroscopy are able to size and analyze on-line particles ranging in size from a few tens of nm to a few μm (e.g. Carson et al., 1997; Ge et al., 1998). However, obtaining quantitative measurements is still challenging (Mur-
10 phy et al., 1998). An alternative is to measure simultaneously but independently the aerosol size distribution, chemical composition and mixing state. The consistency of the various complementary analytical techniques needed can be evaluated by closure experiments.

This work focuses on the size-segregated aerosol chemical composition observed
15 during the first MINATROC (MINeral dust And TROpospheric Chemistry) field experiment at Mte Cimone, Italy (2165 m a.s.l.). We investigate how well the aerosol mass can be described as a mixture of the measured organic and inorganic aerosol components in the sub- and super-μm aerosol fractions. For this, we compare the aerosol size-segregated mass concentration determined from gravimetric measure-
20 ments (m_{GM}) with the aerosol volume calculated particle size distribution measurements, from which we derive the aerosol mass estimate m_{SD}. The aerosol size-segregated mass concentration determined from chemical analyses (m_{CA}) is compared to m_{GM} and m_{SD}. The uncertainties associated with each of the methods are quantified, and the differences between these independent estimates compared
25 to these uncertainties.

This mass closure experiment allows us to determine whether in various synoptic situations the aerosol chemical composition changed significantly with regard to the uncertainties. In particular, we describe the changes in aerosol anthropogenic components' size distribution in a long-range transported desert dust plume.

2. Experimental set-up

2.1. Site and meteorology

The measurements were made between 4 June and 4 July 2000 at the CNR Monte Cimone station (MTC, 44°11′ N–10°42′ E, 2165 m a.s.l.). MTC is located on the high-
5 est summit of the Northern Appennines, and experiences long range transport of air masses from Europe, the Mediterranean basin, and Africa, with on average 5 major dust outbreaks per year (Bonasoni et al., 1996). Ancillary measurements include meteorology, CO_2 and O_3 (Bonasoni et al., 1996, 2000). During the experiment, hourly mean temperature, wind speed and relative humidity averaged 9.5°C (range 4–18°C),
10 5.6 m s^{-1} (range 1–20 m s^{-1}), and 74% (range 1–100%), respectively. Average diurnal variations in CO_2 concentration and standard deviation show that in summer during daytime, surface thermal winds cause up-slope flow that transports possibly polluted low altitude air to MTC (Fig. 1).

2.2. Aerosol mass concentration and chemical composition

15 ### 2.2.1. Sampling

Aerosol was sampled from the terrace of the MTC station situated about 3 m above ground. Size-segregated aerosol was collected at ambient relative humidity over 11-hour periods (10:00–21:00, and 22:00–09:00 UTC) using a low-pressure 6-stage Berner impactor (LPI 80/0.05) loaded with half foils of aluminum and half foils of Ted-
20 lar™. At the nominal flow rate of 80 L/min, the 50% aerodynamic cut-off diameters of this impactor are 0.05, 0.14, 0.42, 1.20, 3.46 and 10 μm for stages 1 to 6, respectively. To accumulate more material, aerosol was also collected through PM10 inlets on a 12 h basis with a high-volume sampler (Hi-Vol, 500 L/min) and for several days or night using a virtual impactor built at the Joint research Centre (JRC) based on Loo
25 and Cork's (1988) design. At the flow rate of 20.0 L/min used during this experiment,

the virtual impactor's 50% cut-off is 1.50±0.1 μm aerodynamic diameter. The Hi-Vol sampler was loaded with ashless cellulose filters (Whatman 41). The virtual impactor sampled on pre-fired quartz fiber filters (Schleicher & Schuell QF20).

2.2.2. Analyses

Low-pressure impactor stages 1–5 were analyzed. The half foils of aluminum were used for gravimetric measurements of samples collected during the 17/06–04/07 period and for the analysis of organic carbon (OC) and black carbon (BC) of samples collected over the whole campaign period. They were weighed with a micro-balance (Sartorius, MC5) at RH = 23±3% and T = 24±1°C (Putaud et al., 2000). The mass of carbon collected on the aluminum foils was determined using a thermal method (Evolved Gas Analysis, EGA), where samples are exposed successively to 5 increasing temperature plateaus up to 650°C in an oxygen-free carrier gas, and then in an oxygen-rich carrier gas at 650–750°C (Putaud et al., 2000). The carbon evolved at T<650°C in He is defined as OC but contains also carbonate, and the fraction evolved at T>650°C in the oxidizing carrier gas is expected to be black carbon (BC). It appeared that the phenomenon of charring was particularly acute when analyzing samples collected on aluminum foils. The amplitude of the charring effect was assessed over 20 samples collected with the same Berner impactor at the same place at MTC in August 2001. Each sample was divided into two half foils, one of which was exposed at 340°C for 2 h in an oxidizing carrier gas (He:O_2 80:20). This thermal treatment was shown to remove most of the OC susceptible to be charred (Cachier et al., 1989). Both half foils were then analyzed using our routine method. BC was determined from the treated aliquot, and the difference in OC between the treated and not treated aliquot was interpreted as charred OC. The regression between the BC mass (μg) found on the treated half foil vs. the BC mass found on the non-treated half foil ($BC_{treated}$ = 0.60 $BC_{non-treated}$, R^2 = 0.97, n = 20) was used to correct the BC data obtained from the non-treated samples collected during the Minatroc campaign.

Tedlar half foils were extracted in 6 mL of ultra-pure water (Millipore Organex system)

and analyzed by ion chromatography (Dionex 500) for Na^+, NH_4^+, K^+, Mg^{2+}, Ca^{2+}, acetate, formate, methanesulfonate (MSA), pyruvate, Cl^-, NO_2^-, NO_3^-, SO_4^{2-}, oxalate and for total water-soluble organic carbon (WSOC) with a Shimadzu TOC-5000A analyzer.

Four quartz filter collected with the virtual impactor were extracted in 6 ml of ultrapure water. The extracts were concentrated to dryness and recovered with 1ml of deuterated water for HNMR analysis. Spectra were recorded at 400 MHz in a 5 mm probe, with a Varian Mercury 400 spectrometer. A pre-saturation pulse sequence was adopted for suppression of the HDO signal (Decesari et al., 2000).

Cellulose filters collected with the Hi-Vol sampler were used for mineral dust quantification. Aliquots of filters were ashed at 600°C for 8 h in quartz crucibles after extraction of water soluble species in mQ™water. The residue, defined as mineral dust, was weighed using a microbalance (Sartorius, MC5). Amounts of mineral dust significantly higher than the blank level (1.0 ± 0.8 $\mu g/cm^2$) were observed in 90% of the analyzed samples.

2.2.3.   Definition of the aerosol components

Except for NH_4^+, NO_3^- and BC concentrations, which were directly obtained from measurements, the main aerosol components were defined as a combination of the analyzed species. The regressions between K^+, Mg^{2+}, Ca^{2+} and SO_4^{2-} on one side and Na^+ on the other side indicate a common source for Na^+ and Mg^{2+} at MTC (sea spray) but not for K^+, Ca^{2+} and SO_4^{2-}. Consequently, sea salt was calculated as the sum of Na^+, Mg^{2+}, Cl^-. The sea salt fractions of K^+, Ca^{2+} and SO_4^{2-} were calculated from the measured Na^+ concentrations and a standard sea water composition. The sea salt SO_4^{2-} fraction was subtracted to measured SO_4^{2-} to get non-sea salt sulfate ($nssSO_4^{2-}$). The dust component was obtained from the regressions between Ca^{2+} and ash found in the Hi-Vol samples. Different correlations were observed between Ca^{2+} and mineral dust for periods with and without mineral dust (Fig. 2). The equations of the regres-

sions:

$$\text{mineral dust} = 5.6 \times \text{nssCa}^{2+}, \text{ for non Saharan dust periods} \qquad (1a)$$

$$\text{mineral dust} = 15.0 \times \text{nssCa}^{2+}, \text{ for the Saharan dust period} \qquad (1b)$$

were used to estimate the amount of mineral dust in each stage of the impactor for
5 each period, based on measured amounts of Ca^{2+}. The water soluble organic matter
(WSOM) was derived from measured WSOC using a mean molecular-to-carbon mass
ratio equal to 1.9, corresponding to the raw molecular formulas for WSOM derived by
HNMR functional group analysis (Fuzzi et al., 2001). Non-water soluble organic matter
(NWSOM) was estimated as:

10 $$\text{NWSOM} = 1.2(\text{OC} - \text{WSOC}). \qquad (2)$$

The 1.2 molecular-to-carbon mass ratio is the lower limit reported for urban organic
matter (Gray et al., 1986) and corresponds to large saturated hydrocarbons. For each
sample, the "unknown" fraction was calculated as the difference between the aerosol
mass m_{GM} or m_{SD} and the sum of the quantified aerosol components m_{CA}.

15 2.2.4.   Uncertainties

The weighing precision was ±2 μg and the standard variation of the aluminum blank
foils ±10μg (n=5). The precision of OC and BC determination was ±8%. The un-
certainty in the slope of the regression between the BC mass from the non-treated
aliquots and the BC mass from the treated aliquots was ±0.03 (95% confidence level).
20 Blank variability for the OC and BC fraction were ±1.7 and ±0.3 μg foil^{-1}, respec-
tively (n=15). Uncertainties in ion chromatography and WSOC measurements were
estimated to ±5%. The precision of the water volume used to extract the samples
was ±0.04 mL. Blank variability for Na^+, NH_4^+, K^+, Mg^{2+}, Ca^{2+}, Cl^-, NO_3^-, SO_4^{2-}, and
WSOC were ±48, ±12, ±17, ±3, ±23, ±30, ±70, ±28, and ± 200 μg L^{-1}, respectively
25 (n=25). The random uncertainty of the molecular mass - to - carbon mass ratios were

4103

Title Page

Abstract   Introduction

Conclusions   References

Tables   Figures

◀   ▶|

◀   ▶

Back   Close

Full Screen / Esc

Print Version

Interactive Discussion

Size-segregated aerosol mass closure and chemical composition

J.-P. Putaud et al.

Title Page

Abstract | Introduction

Conclusions | References

Tables | Figures

⏮ | ⏭

◀ | ▶

Back | Close

Full Screen / Esc

Print Version

Interactive Discussion

arbitrary set to ±0.1 for both WSOM and NWSOM, because eof the lack of data regarding the variability of these ratios. The uncertainty in the slope of the regression between ash and $nssCa^{2+}$ masses measured from the Hi-Vol filters was ± 2.1 for the 4 June–2 July period, and ± 1.73 for the 3–4 July period (95% confidence level). Finally,

5   based on measurements performed later with an identical impactor, the uncertainty in the sampling flow rate was estimated to ± 10%. Tables 1 and 2 show how evolve the relative mean random uncertainties in each aerosol component and in the mass concentration estimates m_{CA}, m_{GM}, and m_{SD}, when sources of errors such analyses, blank variability, conversion from species to aerosol components, and air volume deter-

10 mination., are successively introduced. The law of propagation of errors (3) was used to combine absolute uncertainties associated with the determination of non-correlated parameters. According to the law of propagation of errors, the random error S(y) of a variable y calculated as a function of n non-correlated parameters x_i, y = f (x_1,..., x_i, ...,x_n), can be approximated by:

15 $$S^2(y) = \Sigma\{df/dx_i(x_1, \ldots, x_i, \ldots, x_n)S(x_i)\}^2, \qquad (3)$$

where (df/dx_i) represents the partial derivative of f with respect to x_i and $S(x_i)$ is the absolute uncertainty of parameter x_i. For correlated parameters, such as the various components of sea salt, absolute uncertainties were conservatively added. Uncertainties for the sub-μm aerosol range is also the sum of uncertainties for stages 1-3 of the

20 impactor, and uncertainties for the super-μm range the sum of uncertainties for stages 4–5. The main source of uncertainty for the gravimetric method (m_{GM}) was the variability of the blank masses. For most aerosol components, the main source of random error is blank variability as well. Analytical precision is the largest source of random error only for NH_4^+, $nssSO_4^{2-}$, and BC in the aerosol sub-μm fraction, and for NWSOM

25 in both the super- and sub-μm fraction. The large uncertainty in NWSOM derives from the fact that NWSOM was calculated as the difference between two quantities (2), which were for numerous samples much larger than NWSOM itself. The overall random uncertainty in the determination of the aerosol mass from chemical analysis

(m_{CA}) was dominated by uncertainties in OM (OM = WSOM + NSOM) and nssSO$_4^{2-}$ for the sub-μm fraction, and by uncertainties in OM and dust for the super-μm fraction.

In addition to random uncertainties, systematic errors can occur, related to inaccurate sampling or analytical techniques. Aerosol sampling with low-pressure impactors
5 is suspected to be affected by negative artifacts, due to the volatilization of semi-volatile particulate species. During Minatroc, sub-μm aerosol was collected and analyzed online at MTC using an artifact free sampler made of a wet annular denuder (WAD) combined with a steam jet aerosol collector (SJAC) built by ECN, Petten (Keuken et al., 1988; Khlystov et al., 1995). The correlation between the sub-μm NO$_3^-$ concentrations
10 calculated from the impactor samples and the WAD-SJAC concentrations averaged over the impactor sampling time show that the low-pressure impactor did not lead to systematically lower concentrations than the artifact free sampler. This suggests that no significant loss of semi-volatile compounds occurred in the low-pressure impactor in the conditions encountered during this campaign. Possible losses of coarse dust
15 particles into the impactor are discussed in Sect. 3.

The determination of OM concentrations is also affected by possibly large systematic errors due to the lack of accurate data regarding the molecular mass-to-carbon mass ratio of organic aerosol in NWSOM, and to the uncertainties involved by the assumptions needed to interpret HNMR data to determine the mean raw formula of WSOM.
20 Such systematic uncertainties are very difficult to estimate.

2.3. Aerosol physical properties

2.3.1. Measurements

All instruments sampled from the same PM10 inlet located at 4 m above the terrace floor (Van Dingenen et al., this issue). Particle size distributions at 5±5% RH were
25 measured with a 10-min time resolution in the size range 6–600 nm using a Vienna type differential mobility analyzer (DMA). Particle size distributions for aerodynamic diameters greater than 0.3 μm were measured using a Grimm 1.108 optical particle

Size-segregated aerosol mass closure and chemical composition

J.-P. Putaud et al.

Title Page

Abstract · Introduction

Conclusions · References

Tables · Figures

◀ · ▶|

◀ · ▶

Back · Close

Full Screen / Esc

Print Version

Interactive Discussion

counter (OPC). The optical diameters determined by the OPC are converted to geometric diameters assuming spherical particles. A tandem-DMA was used to measure the aerosol growth factor from 0 to 90% RH at particle diameters of 10, 20, 50, 100 and 200 nm. Aerosol absorption coefficient was measured with an aethalometer ™(Magee AE-1).

2.3.2. Data processing

Particle number size distributions measured with the DMA and the OPC agreed well in the overlapping 300–600 nm range (Van Dingenen et al., this issue). Volume size distributions were calculated assuming that aerosol particles were spheres with a diameter equal to that measured by the instruments. DMA rather than OPC data were considered in the 300–600 nm range, but this choice had no significant influence (<1%) on the aerosol volume determination. Volume size distributions in the size range 6 nm–10 μm were averaged over the impactor sampling periods.

2.3.3. Uncertainties

The possible error in DMA sizing due to the uncertainty in the air flow rates (±5%) are −7, +5% of the particle diameter. The comparison with a condensation particle counter (CPC) indicates that the uncertainty in DMA counting was ±2% (95% confidence level). According to the manufacturer, the reproducibility of the Grimm 1.108 OPC in particle counting is ±2%. We assumed random uncertainties in particle sizing to ±10% and ±20% out and during the desert dust advection period, respectively. The overall random uncertainty in aerosol volume determination was controlled by the precision in particle sizing.

3. Results and discussion

3.1. Mass closure

3.1.1. Comparison between the aerosol mass concentrations derived from gravimetric measurements and aerosol volume derived from particle size distributions.

Such a comparison requires first the conversion of the 50% aerodynamic cut-off diameters of the impactor operated at ambient temperature to geometric diameters measured in dry conditions in the particle sizing instruments. The aerodynamic diameter of a particle at ambient relative humidity D_a and its geometric diameter at 0% relative humidity D_g are linked by the relationship:

$$D_g = 1/GF_a \times [D_a/(d_a)^{1/2}] \times [Cc_1/Cc_d]^{1/2}, \tag{4}$$

where GF_a and d_a are the particle growth factor and density at ambient relative humidity, and Cc_1 and Cc_d are the slip correction factors for spheres with diameters D_a and $D_a \times d_a^{-1/2}$, respectively. Variations in the slip correction factors are significant for particle diameters <0.2μm only. They were neglected in the conversion from aerodynamic to geometric cut-off diameters.

The aerosol density at ambient RH (d_a) can be calculated by:

$$d_a = (d_0 + (GF_a^3 - 1)d_w)/GF_a^3, \tag{5}$$

where d_0 is the aerosol density at 0% relative humidity, d_w is the density of water (=1.0) and GF_a the aerosol growth factor at ambient relative humidity.

Aerosol growth factor at 90% RH (GF_{90}) were measured continuously at MTC during this campaign (Van Dingenen et al., this issue). From the GF_{90} values averaged over the impactor sampling periods, the fractions of hygroscopic (α) and hygrophobic (1-α) aerosol components were estimated assuming that (1) hygroscopic aerosol behave

4107

Title Page

Abstract | Introduction

Conclusions | References

Tables | Figures

◄◄ | ►►

◄ | ►

Back | Close

Full Screen / Esc

Print Version

Interactive Discussion

like $(NH_4)_2SO_4$, and (2) hydrophobic aerosol do not grow at any RH, and the GF of a mixture can be calculated according to the formula (Virkkula et al., 1999):

$$GF_{90}^3 = \alpha GF_{90\,scopic}^3 + (1 - \alpha)GF_{90\,phobic}^3. \tag{6}$$

The coefficient α calculated from (6) was used to estimate the aerosol growth factor at ambient relative humidity, based on the above mentioned assumptions (1) and (2):

$$GF_a^3 = \alpha GF_{a\,scopic}^3 + (1 - \alpha)GF_{a\,phobic}^3. \tag{7}$$

For each impactor sample, the geometric diameter $D_g(4)$ corresponding to the 50% cut-off diameter of stage 4 (1.2 μm aerodynamic diameter) was calculated for the dry aerosol density values 1.0, 1.5, 2.0 (this range of values largely covers the possible atmospheric dry aerosol density). This equivalent geometric diameter $D_g(4)$ was found to be on average 0.95 ± 0.12 μm. The aerosol mass concentration measured on stages 1–3 of the impactor was then compared to the aerosol volume integrated up to the geometric diameter $D_g(4)$ (Fig. 4a), and the aerosol mass concentration measured on stages 4 and 5 of the impactor to the aerosol volume integrated from to the geometric diameter $D_g(4)$ to 10 μm (Fig. 4b). For the sub-μm aerosol range, a good correlation is observed between the gravimetrically measured mass m_{GM} and the aerosol volume, independently of the *a priori* assumed dry aerosol density. The slope of the regression suggests that the density of the dry aerosol was in the range 1.55 ± 0.12 (95% confidence level) at MTC during the Minatroc campaign. For the periods when gravimetric measurements are not available, this regression together with the size distribution measurements performed on these days were use to estimate the sub-μm aerosol mass m_{SD}. The comparison between gravimetrically measured mass and aerosol volume was carried out for each of the 3 sub-μm aerosol fractions resolved by the low-pressure impactor. A reasonable agreement could be found by assuming that the 50% cut-off diameter of stage 3 was 0.26 instead of the nominal 0.42 μm value. Regarding the aerosol super-μm range, no correlation appears between the gravimetrically measured mass and the aerosol volume (Fig. 4b). The regression

Size-segregated aerosol mass closure and chemical composition

J.-P. Putaud et al.

Title Page

Abstract	Introduction
Conclusions	References
Tables	Figures

◄◄   ►►

◄   ►

Back   Close

Full Screen / Esc

Print Version

Interactive Discussion

Size-segregated aerosol mass closure and chemical composition

J.-P. Putaud et al.

indicates that the discrepancies between super-μm aerosol mass and volume are not systematically due to losses of coarse particles into the impactor. It shows that coarse particle sampling with the low-pressure impactor and/or counting with the OPC were affected by random uncertainties (sampling artifacts into the impactor, error in particle sizing, etc...), which were not adequately accounted for.

3.1.2. Comparison between aerosol mass concentrations derived from gravimetric measurements and chemical analysis

Sub- and super-μm aerosol mass concentrations derived from gravimetric measurements (m_{GM}) and chemical analyses (m_{CA}) are compared in Figs. 5a and 5b, respectively. A good correlation appears for the sub-μm aerosol fraction (slope = 0.89, R^2 = 0.82), but not for the super-μm fraction (slope = 0.65, R^2 = 0.58). To compare m_{GM} and m_{CA} with regard to the uncertainty of each method, the absolute difference between two methods $\Delta = |m_{CA} - m_{GM}|$ was compared with the uncertainty in this difference ($S\Delta$), which can be estimated according to Eq. (3) as:

$$S(\Delta)^2 = S(m_{CA})^2 + S(m_{GM})^2. \tag{8}$$

Mean relative uncertainties $\sigma(\Delta)$ in the difference and relative differences between the two methods $\delta(m_{GM}, m_{CA})$, respectively defined by:

$$\sigma(\Delta) = S(\Delta)/m \tag{9}$$

$$\delta(m_{GM}, m_{CA}) = (\Delta)/m, \tag{10}$$

where m = average (m_{GM}, m_{CA}), are listed in Table 3. For the sub-μm aerosol fraction, $\delta(m_{GM}, m_{CA}) < \sigma(\Delta)$, which means that the difference between m_{GM} and m_{CA} are not statistically significant. This shows that the quantified aerosol components adequately describe the sub-μm aerosol mass. In contrast, for the super-μm fraction, $\delta(m_{GM}, m_{CA}) > \sigma(\Delta)$, which indicates that differences in aerosol the aerosol mass determined from chemical analyses g(m_{GM}) compared to gravimetry (m_{CA}) were larger

than the estimated random errors. This suggests that systematic errors might not have been adequately taken into account.

3.2. Aerosol chemical composition in various particle size classes and air masses

Numerous parameters such as relative humidity, CO_2 concentration and standard deviation, aerosol absorption coefficient (B_{abs}) indicate that during the Minatroc campaign, MTC was reached from about 08:00 to 21:00 UTC by air masses coming from low altitude and therefore possibly affected by local pollution. Impactor measurements show also that aerosol concentration was on average 30% higher during day-time compared to night-time, mainly due to enhanced mass concentrations in stages 2 ($0.14 < D_a < 0.42\,\mu$m) and 5 ($3.46 < D_a < 10\,\mu$m). However, the chemical composition in each size fraction did not vary much between night and day (Fig. 6). Particles with $D_a < 0.14\,\mu$m (stage 1) were mainly made of carbonaceous species. The contribution of carbonaceous components decreased for stages 2 and 3, and increased again for stages 4 and 5. This was mainly due to variations in the NSWOM contribution, since the one of WSOM was quite similar in each size fraction (22±7%). $NssSO_4^{2-}$ and NH_4^+ were mainly found into sub-μm particles, whereas NO_3^- was more equally distributed over the 5 size fractions. Sea-salt and dust were almost exclusively present in the super-μm aerosol fraction. The air masses reaching MTC over the impactor night-time sampling periods (21:00–09:00 UTC) were classified into 5 categories (W-Europe, NW-Europe, E-Europe, Mediterranean) based on 3-D back trajectories calculated by Balkanski et al. (2003) and observation of super-μm particle number (indicating the Saharan dust outbreak). The sub- and super-μm aerosol chemical compositions determined from nighttime impactor samples corresponding to air masses of clearly identified origins are indicated in Table 4 and 5 and presented in Fig. 7. It should be noted that the variability in the composition of both size fractions is high, even in air masses from the same origin. However, some peculiarities in sub-μm aerosol composition can be noticed, which are significant with respect to uncertainties in each component quantification (Table 4). The average contribution of NO_3^- to the sub-μm aerosol mass

Size-segregated aerosol mass closure and chemical composition

J.-P. Putaud et al.

Title Page

Abstract	Introduction
Conclusions	References
Tables	Figures

◀ | ▶|

◀ | ▶

Back | Close

Full Screen / Esc

Print Version

Interactive Discussion

concentration was >20% for 3 among 5 samples collected in air masses from NW-Europe origin, which is much higher than what was observed in any other type of air mass. In contrast, sub-μm aerosol in air masses from E-Europe origin was for more than 50% made of carbonaceous matter, due to specially high contribution of NWSOM and BC. The molar ratio NH_4^+ / (NO_3^- + 2× $nssSO_4^{2-}$) also suggests that sub-μm was acidic in air masses from E-Europe and Mediterranean origin only. In air masses from Mediterranean origin, $nssSO_4^{2-}$ was on average the main single component, and could make up to 50% of the aerosol mass in some samples. Despite a large uncertainty, it appears that mineral dust was a major component of the sub-μm aerosol during the Saharan dust outbreak. However, no Ca^{2+} was observed in the sub-μm aerosol collected with the SJAC. The occurrence of mineral dust in the sub-μm aerosol fraction might therefore result form the bouncing of non-sticky particles into the impactor. The super-μm aerosol chemical composition is presented is Table 5. It should be kept in mind that chemical closure was not reached for the super-μm fraction, which indicates that overall uncertainties were larger than estimated. It was characterized by a rather constant contribution of sea-salt with regard to uncertainties. The large contribution of NO_3^- observed for air masses with NW-European origin (20±6%) and Mediterranean origin (15%) were not significantly different from others with respect to uncertainties. The contribution of mineral dust to the super-μm aerosol mass concentration was the highest during the Saharan dust outbreak. During this event, the $nssSO_4^{2-}$/$nssCa^{2+}$ ratio observed at MTC in the super-μm aerosol averaged 0.4 ± 0.1. Alpine glacier ice-cores (Schwikowski et al., 1995) and IC analyses of Saharan sand fine grain samples suggest that the SO_4^{2-}/Ca^{2+} mass ratio should be about 0.4-0.6 in pure Saharan dust. This shows that super-μm $nssSO_4^{2-}$ was probably of pure Saharan origin during the dust outbreak. In contrast, large amounts of excess-SO_4^{2-} were still present in the sub-μm fraction. It can therefore be stated that coarse particles from Saharan and fine particles from anthropogenic origin were certainly externally mixed during the Saharan dust outbreak, and that no significant oxidation of SO_2 onto mineral dust particles occurred in the Saharan dust plume. On the other hand, NO_3^- was predominantly in the

coarse fraction (coarseNO_3^-/total NO_3^- = 88±1%). This value is not significantly higher than the value observed in air masses from Mediterranean and E-Europe origin, in which large contribution of dust to the super-μm aerosol mass was also observed, but significantly higher that in air masses from W-and NW-Europe origin (coarseNO_3^-/total

5   NO_3^- = 47±23%). This suggests that in presence of coarse dust particles, NO_3^- shifts to the aerosol super-μm fraction due to the adsorption of HNO_3 onto dust particles, leading to the displacement to the right of the equilibrium:

$$NH_4NO_3 \longleftrightarrow HNO_3 + NH_3 \qquad (11)$$

4. Conclusions

10   For the Minatroc campaign at MTC, the mean random uncertainties in the determination of sub- and super-μm aerosol mass concentrations from gravimetric measurements (m_{GM}), chemical analyses (m_{CA}), and particle size distribution measurements (m_{SD}) ranged between ±14 and ±29%. The main sources of random uncertainties were blank variability for m_{GM} and m_{CA}, and particle sizing for m_{SD}. Additional possi-

15   ble systematic error affecting mainly the conversion factors used to determine WSOM and NWSOM concentrations cannot be estimated. The comparison of m_{CA} with m_{GM} and m_{SD} shows that average differences were within experimental uncertainties for the sub-μm aerosol fraction. This indicates that within experimental uncertainties, the sub-μm aerosol was made of the ionic, carbonaceous and refractory components

20   we quantified. In contrast, mass closure was not obtained for the aerosol super-μm fraction. This shows that the sources of random and/or systematic errors associated with the determination of m_{CA}, m_{GM} and m_{SD} for the super-μm aerosol fraction were not fully understood. Taking into account analytical uncertainties, we found significant differences in the sub-μm aerosol composition in air masses from different origins.

25   The largest contribution of NO_3^- was observed in air masses from NW-Europe origin, whereas more than 50% of the sub-μm aerosol mass was made of carbonaceous

Size-segregated aerosol mass closure and chemical composition

J.-P. Putaud et al.

components in air masses from E-Europe origin. The difference in sub- and super-μm chemical composition during the Saharan dust outbreak suggests that Saharan dust and anthropogenic particles were externally mixed. No interaction between SO_2 and dust could be detected from our measurements. In contrast, the displacement of NO_3^-

5 towards the aerosol super-μm fraction in presence of dust coarse particles suggests a significant interaction of HNO_3 with dust particles. This suggests that the interaction of secondary aerosol precursors with pre-existing primary particles should be taken into account in secondary aerosol formation modeling.

References

Balkanski, Y., Bauer S. E., Van Dingenen R., Bonasoni P., Schulz M., Fischer H., Gobbi G. P., Hanke M., Hauglustaine D., Putaud J. P., Stohl, A., and Raes, F.: The Mt Cimone, Italy, free tropospheric campaign: principal characteristics of the gaseous and aerosol composition
15 from European pollution, Mediterranean influences and during African dust events, Atmos. Chem. Phys. Discuss., 3, 1753–1776, 2003.

Bonasoni, P., Colombo, T., Lenaz, R., Giovanelli, G., Evangelisti, F., Ravegnani, F., Santaguida, R., and Tesi, G.: Effect of Saharan dust transport on ozone and carbon dioxide concentrations – The impact of African dust across the Mediterranean, Envir. Sci. Technol. Lib. Kluwer
20 Academic Publ., 313–322, 1996.

Bonasoni, P., Stohl, A., Cristofanelli, P., Calzolari, F., Colombo, T., and Evangelisti, F.: Background ozone variations at Mt. Cimone, Atmos. Environ. 34, 5183–5189, 2000.

Cachier, H., Bremond M. P., and Buat-Ménard, P.: Determination of atmospheric soot carbon with a simple thermal method, Tellus 41B, 379–390, 1989.
25 Carson, P. G., Johnston, M. V., and Wexler, A. S.: Real time monitoring of the surface and total composition of atmospheric particles, Aeros. Sci. and Technol., 26, 291–300, 1997.

Decesari, S., Facchini, M. C., Fuzzi, S., and Tagliavini, E.: Characterization of water-soluble organic compounds in atmospheric aerosol: A new approach, J. Geophys. Res. 105, 1481–1489, 2000.

Size-segregated aerosol mass closure and chemical composition

J.-P. Putaud et al.

Title Page

Abstract | Introduction

Conclusions | References

Tables | Figures

◄ | ►

◄ | ►

Back | Close

Full Screen / Esc

Print Version

Interactive Discussion

Fuzzi, S., Decesari, S., Facchini, M.C., Matta, E., Mircea, M., and Tagliavini, E.: A symplified model of the water soluble organc component of atmospheric aerosol, Geophys. Res. Lett. 20, 4079–4082, 2001.

Ge, Z., Wexler, A. S., and Johnston, M. V.: Laser desorption/ionization of single ultrafine multi-component aerosols, Environ. Sci. and Technol., 32, 3218–3223, 1998.

Gray, H. A., Cass, R. G., Huntzicker, J. J., Heyrdahl, E. K., and Rau, J. A.: Characteristics of atmospheric organic and elemental carbon particle concentrations in Los Angeles, Environ. Sci. Technol. 20, 580–589, 1986.

IPCC, Climate Change 2001: The scientific basis. Contribution of Working Group I to the third assessment report of the Intergovernmental Panel on Climate Change [Houghton, J.T., Y. Ding, D.J. Griggs, M. Noguer, P.J. van der Linden, X. Dai, K. Maskell, and C.A. Johnson (eds.)]. Cambridge University Press, Cambridge, United Kingdom and New York, NY, USA, 881 pp, 2001.

Keuken, M. P., Schoonebeeek, C. A. M., van Wensveen-Louter, A., and Slanina, J.: Simultaneous sampling of NH_3, HNO_3, HCl, SO_2, and H_2O_2 in ambient air by wet annular denuder system, Atmos. Environ. 22, 2541–2548, 1988.

Khlystov, A., Wyers G. P., and Slanina, J.: The steam jet aerosol collector, Atmos. Environ. 29, 2229–2234, 1995.

Loo, B. W. and Cork, C. P.: Development of a high efficiency virtual impactor, Aerosol Sci. Technol.9, 167–176, 1988.

Murphy, D. M., Thomson, D. S., and Mahoney, M. J.: In situ measurement of organics, meteoritic material and other elements in aerosol at 5 to 19 km, Science, 282, 1664–1669, 1998.

Putaud, J. P., Van Dingenen, R., Mangoni, M., Virkkula, A., Raes, F., Maring, H., Prospero, J. M., Swietlicki, E., Berg, O. H., Hillamo, R., and Mäkelä, T.: Chemical mass closure and assessment of the origin of the submicron aerosol in the marine boundary layer and the free troposphere at Tenerife during ACE-2, Tellus 52B, 141–168, 2000.

Schwikowski, M., Seibert, P., Baltensberger, U., and Gäggeler, H. W.: A study of an outstanding Saharan dust event at the high-alpine site Jungfraujoch, Switzerland, Atmos. Environ. 29, 1829–1842, 1995.

Van Dingenen, R., Putaud, J. P., and Raes, F.: Physical aerosol properties and their relation to air mass origin at Monte Cimone (Italy) during the first MINATROC campaign, this issue.

Virkkula, A., Van Dingenen, R., Raes, F., and Hjorth, J.: Hygroscopic properties of aerosol

ACPD

3, 4097–4127, 2003

Size-segregated aerosol mass closure and chemical composition

J.-P. Putaud et al.

Title Page

Abstract	Introduction
Conclusions	References
Tables	Figures

◄◄ ►►

◄ ►

Back Close

Full Screen / Esc

Print Version

Interactive Discussion

© EGU 2003

formed by oxidation of limonene, α-pinene and β-pinene. J. Geophys. Res. 104, 3569–3579, 1999.

Size-segregated aerosol mass closure and chemical composition

J.-P. Putaud et al.

Title Page	
Abstract	Introduction
Conclusions	References
Tables	Figures

◄◄	►►
◄	►
Back	Close

Full Screen / Esc

Print Version

Interactive Discussion

© EGU 2003

Size-segregated aerosol mass closure and chemical composition

J.-P. Putaud et al.

Title Page

Abstract | Introduction

Conclusions | References

Tables | Figures

|◄ | ►|

◄ | ►

Back | Close

Full Screen / Esc

Print Version

Interactive Discussion

Table 1. Evolution of the mean relative uncertainties $S(x_i)/x_i$ (%) in sub-μm aerosol component and mass concentrations at MTC when various sources of errors are successively taken into account out of the desert dust advection period. Also indicated are the overall uncertiainty in these parameters for the desert dust advection period and main sources of errors

Period	Sources of error	sea salt	NH4	NO3	nssSO4	WSOM	NWSOM	BC	dust	m_{CA}	m_{GM}	unknown	m_{SD}
Out of desert dust advection	analytical	5	5	5	5	5	60	10	5	8	3	57	12
	analytical + blank variability	156	7	82	6	24	77	12	101	18	14	169	
	analytical + blank variability +conversion factor					25	78		116	19		180	14
	analytical + blank variability +conversion factor + air volume	156	9	83	7	25	78	13	116	19	16	192	14
	main source of error	blank variability	analysis	blank variability	analysis	blank variability	analysis	analysis	blank variability	blank variability	blank variability	blank variability	particle sizing
During desert dust advection	analytical + blank variability +conversion factor + air volume	40	7	74	7	27	44	12	21	17	10	182	14
	main source of error	blank variability	blank variability	blank variability	blank variability	blank variability	analysis	analysis + blank var.	conversion factor	blank variability	blank variability	blank variability	particle sizing

Size-segregated aerosol mass closure and chemical composition

J.-P. Putaud et al.

Title Page

Abstract   Introduction

Conclusions   References

Tables   Figures

◀   ▶|

◀   ▶

Back   Close

Full Screen / Esc

Print Version

Interactive Discussion

Table 2. Same as Table 1 for the super-μm aerosol

Period	Sources of error	sea salt	NH4	NO3	nssSO4	WSOM	NWSOM	BC	dust	m_{CA}	m_{GM}	unknown	m_{SD}
Out of desert dust advection	analytical	7	5	5	9	6	20	10	12	9	3	14	20
	analytical + blank variability	34	30	12	17	54	31	20	33	22	15	55	
	analytical + blank variability +conversion factor					54	32		133	31		61	22
	analytical + blank variability +conversion factor + air volume	36	30	13	19	55	32	21	134	31	15	62	22
	main source of error	blank variability	blank variability	blank variability	blank variability	blank variability	analysis	analysis + blank var.	conversion factor	blank variability	blank variability	blank variability	particle sizing
During desert dust advection		8	24	9	13	37	25	19	8	11	6	140	41
	main source of error	blank variability	blank variability	blank variability	blank variability	blank variability	analysis	analysis + blank variability	conversion factor	blank variability	blank variability	blank variability	particle sizing

Size-segregated aerosol mass closure and chemical composition

J.-P. Putaud et al.

Table 3. Magnitude of the relative differences and uncertainties in the relative difference between m_{CA}, and m_{GM}, in the sub- and super-μm aerosol fractions at MTC

	Sub-μm	Super-μm
Relative difference $\delta(m_{CA}, m_{C_GM}$ between m_{CA} and m_{GM} (%)	17	37
Relative uncertainty $\delta(m_{CA}, m_{C_GM}$ of the difference between m_{CA} and m_{GM} (%)	25	33

Print Version

Interactive Discussion

© EGU 2003

Table 4. Average composition, standard deviation and error of the mean (all in %) for the sub-μm aerosol fraction in air masses from various origins

	# of samples	sea salt	NH_4^+	NO_3^-	nss SO_4^{2-}	WSOM	NWSOM	BC	dust	unknown
average W-Eur	4	0.5	14.	5.5	27.	32.	7.5	6.3	1.8	4.4
stdev		0.3	3.7	4.8	9.7	6.8	7.4	1.4	0.65	13.9
error of the mean		*0.4*	*1.3*	*2.3*	*2.4*	*4.8*	*3.0*	*0.7*	*1.1*	*0.6*
average NW-Eur	5	0.6	15.	19.	22.	22.	3.6	4.7	0.7	13
stdev		0.4	3.3	15.	8.0	7.7	3.7	1.3	0.4	14
error of the mean		*0.4*	*1.2*	*7.0*	*1.7*	*2.9*	*1.3*	*0.4*	*0.4*	*1.4*
average E-Eur	5	0.9	6.9	1.8	22.	22.	28	6.7	7.2	4.8
stdev		0.8	4.6	0.9	5.5	5.3	18	0.6	13	15
error of the mean		*0.6*	*0.3*	*0.7*	*1.7*	*2.9*	*10*	*0.6*	*3.8*	*0.5*
average Med	4	0.6	13.	2.4	36.	24.	10	4.8	2.1	6.1
stdev		0.4	5.6	3.5	13.	9.82	11	2.2	2.1	34
error of the mean		*0.4*	*1.2*	*1.0*	*3.0*	*3.61*	*4.0*	*0.5*	*1.2*	*0.8*
average Dust Plume	2	1.6	9.1	1.2	27.	16	7.4	4.3	23	11
stdev		0.6	2.8	0.1	4.5	8.4	0.8	0.5	6.9	11
error of the mean		*1.8*	*1.2*	*0.7*	*3.4*	*3.3*	*4.2*	*0.6*	*18.7*	*1.9*

Table 5. Same as Table 4 (all in %) for the super-μm aerosol fraction

	# of samples	sea salt	NH_4^+	NO_3^-	nss SO_4^{2-}	WSOM	NWSOM	BC	dust	unknown
average W-Eur	3	4.5	2.2	11	3.9	14	14	2.0	6.0	43
stdev		1.6	0.8	2.7	2.7	2.3	4.1	0.5	4.2	5.7
error of the mean		*4.1*	*0.2*	*5.2*	*0.4*	*2.4*	*6.2*	*0.2*	*4.1*	*6.3*
average NW-Eur	3	6.9	3.4	20	5.3	12	15	2.3	5.6	30
stdev		2.5	1.7	5.6	1.4	1.0	1.4	1.4	3.2	7.3
error of the mean		*6.3*	*0.4*	*9.6*	*0.5*	*2.1*	*6.8*	*0.3*	*3.8*	*4.3*
average E-Eur	5	2.8	1.9	7.1	6.4	8.2	24	2.9	9.3	40
stdev		2.9	1.8	3.6	7.3	3.2	10	1.1	4.5	12
error of the mean		*2.0*	*0.2*	*2.7*	*0.5*	*1.1*	*8.2*	*0.3*	*4.9*	*4.5*
average Med	1	5.1	1.7	16	2.5	6.8	22	0.9	18	28
stdev										
error of the mean		*8.1*	*0.3*	*13*	*0.4*	*2.0*	*17*	*0.2*	*21*	*7.1*
average Dust Plume	2	4.9	0.3	6.3	1.5	6.5	7.0	1.1	73	-0.1
stdev		1.3	0.2	3.0	0.3	4.4	3.6	0.2	6.1	6.9
error of the mean		*5.4*	*0.04*	*3.8*	*0.2*	*1.4*	*4.0*	*0.2*	*60*	*0.02*
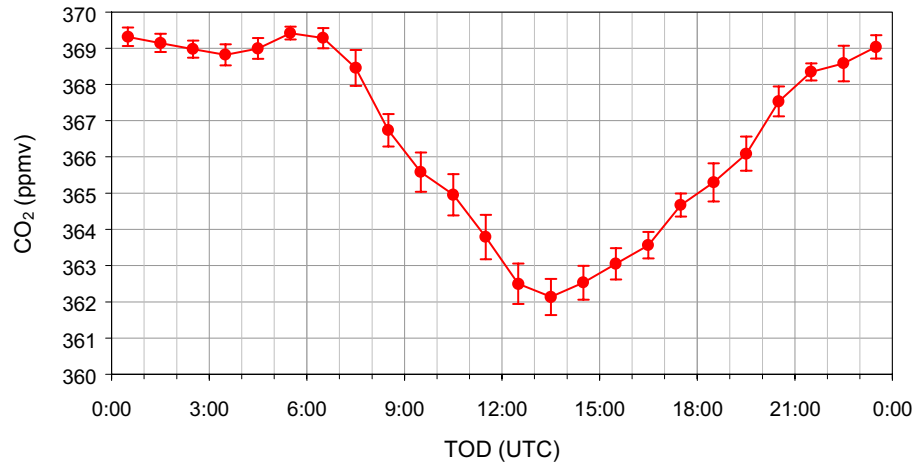
Fig. 1. Mean diurnal variations in CO_2 concentrations at MTC during the 4 June–4 July 2002 period.

Fig. 2. Correlation between ash (considered to be mineral dust) and nss Ca^{2+} in samples collected with a PM10 Hi-Vol sampler and the cascade impactor, respectively. The regression observed out and during the desert dust advection period are shown.

Title Page

Abstract | Introduction

Conclusions | References

Tables | Figures

◄ | ►|

◄ | ►

Back | Close

Full Screen / Esc

Print Version

Interactive Discussion

$$y = 1.01x + 0.02$$
$$R^2 = 0.83$$
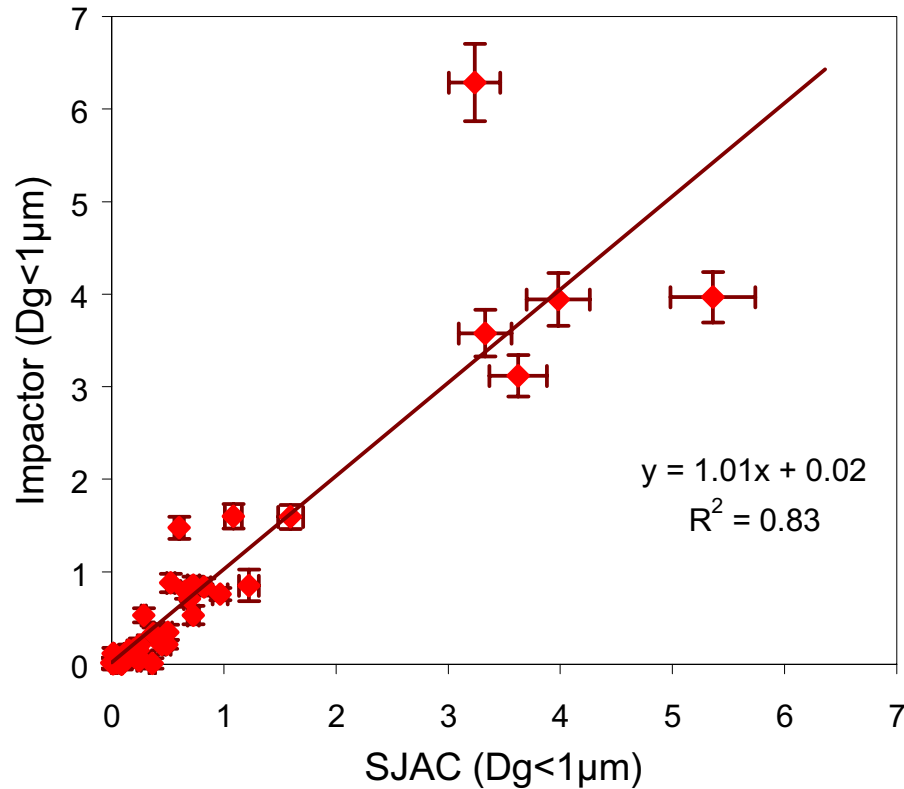
Fig. 3. Correlation between sub-μm NO_3^- concentrations obtained from stages 1-3 of the low-pressure impactor and the artifact free WAD-SJAC combination.
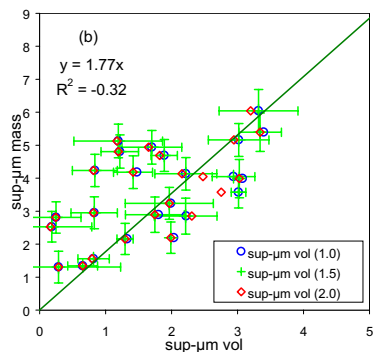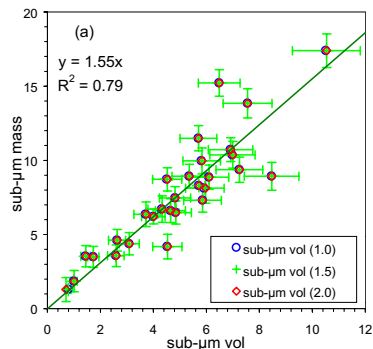
Fig. 4. Correlations between aerosol mass concentrations m_{GM} obtained from the low-pressure impactor and aerosol volume obtained from the DMA and OPC in **(a)** the sub-μm and **(b)** the super-μm aerosol fractions. Data are shown for 3 values of the dry aerosol density (1.0, 1.5, 2.0) considered a priori to convert aerodynamic to geometric diameters. The regression line corresponds to d = 1.5. Error bars indicate random uncertainties associated with m_{GM} and aerosol volume determinations.
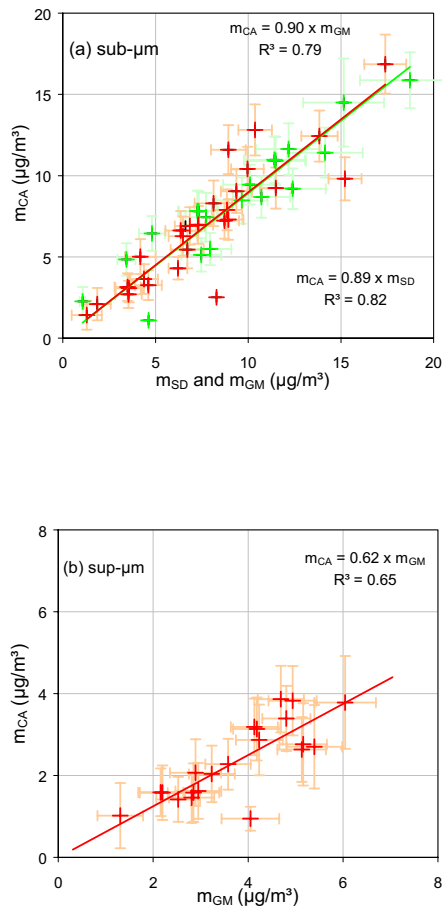
Fig. 5. Correlation between aerosol mass concentrations m_{GM} and m_{CA} obtained from the low-pressure impactor in **(a)** the sub-μm and **(b)** the super-μm aerosol fractions. Error bars indicate random uncertainties associated with m_{GM} and m_{CA}.

Title Page

Abstract | Introduction

Conclusions | References

Tables | Figures

|◄ | ►|

◄ | ►

Back | Close

Full Screen / Esc

Print Version

Interactive Discussion
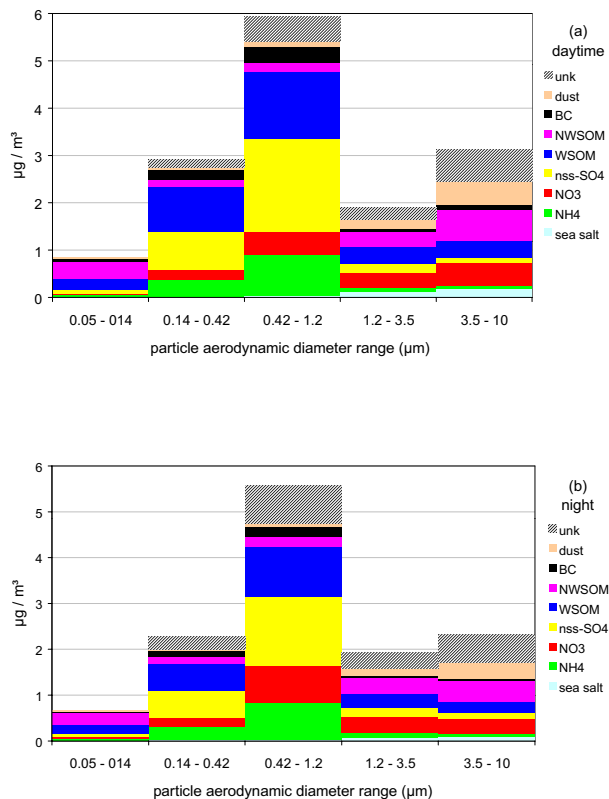
Fig. 6. Mean size-segregated aerosol chemical composition during **(a)** daytime and **(b)** night-time at MTC during the Minatroc campaign, out of the Saharan dust advection period.
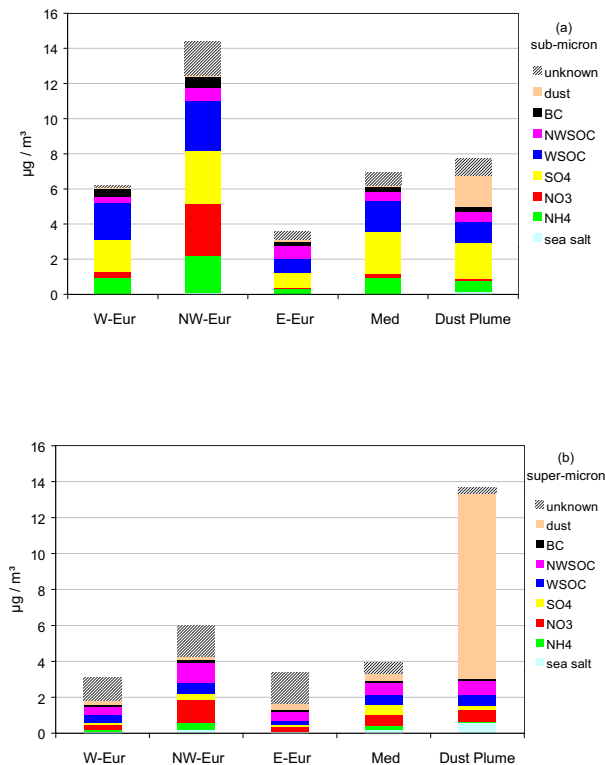
| Title Page |
Abstract	Introduction
Conclusions	References
Tables	Figures
◄◄	►►
◄	►
Back	Close
Full Screen / Esc

Print Version

Interactive Discussion

Fig. 7. Mean **(a)** sub-μm and **(b)** super-μm aerosol component concentrations in air masses from various origins during the Minatroc campaign.